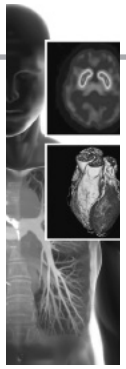

Ultrasound detection of cell death

Ultrasound has been used to detect tissue pathology since the 1960s. Although early studies were limited in terms of their appreciation of biology and the physics of ultrasound backscatter as it related to the biology of cell death, recent investigations combining rigorous and well-controlled biological experimentation and quantitative ultrasound methods have provided valuable information. Studies indicate that ultrasound may be used to detect and potentially quantify cell death *in vitro*, *in situ* and *in vivo* at conventional ultrasound frequencies, higher ultrasound frequencies and using ultrasound microscopy. These studies point to an important role of the cell's nucleus and its configuration in the formation of ultrasound backscatter in addition to cellular morphology.

KEYWORDS: apoptosis ▪ cell death ▪ necrosis ▪ oncolysis ▪ quantitative ultrasound ▪ speckle analysis ▪ spectral analysis ▪ tissue characterization ▪ ultrasound

Gregory J Czarnota[1,2,3,4,5†] & Michael C Kolios[4,5]

[†]Author for correspondence:
[1]Radiation Oncology, Sunnybrook Health Sciences Centre, Ontario, Canada
[2]Department of Radiation Oncology, University of Toronto, 2075 Bayview Avenue, Toronto, Ontario, M4N 3M5, Canada
Tel.: +1 416 480 6100 ext. 7073
Fax: +1 416 480 6002
gregory.czarnota@sunnybrook.ca
[3]Imaging Research, Sunnybrook Health Sciences Centre, Ontario, Canada
[4]Department of Medical Biophysics, University of Toronto, Ontario, Canada
[5]Department of Physics, Ryerson University, Ontario, Canada

Cell death history

Ultrasound is now one of the most common imaging modalities worldwide since it can provide good spatial and temporal imaging resolution at a reasonable cost. In the several decades following the introduction of ultrasound, it has become one the most popular forms for imaging human anatomy in the world. Close to 25% of all imaging procedures are based on ultrasound [1]. However, ultrasound can be susceptible to subjective operator dependence and has relatively poor inherent soft-tissue contrast. Therefore, developments in the field of ultrasound imaging are focused on technological improvements to improve signal-to-noise ratios or on the use of new techniques to increase soft-tissue contrast, such as microbubble contrast agents [2–4], elastography [5,6], applied radiation force imaging [7,8] and shear wave imaging [9,10]. One way to achieve operator independence is by performing quantitative analysis of backscatter data prior to image formation. This type of analysis forms the basis of classical ultrasound tissue characterization [11–20]. Research on the ultrasound detection of cell death can be considered a form of tissue characterization and is based on two premises: as the ultrasound wavelength approaches the size of the cell, the tissue scattering characteristics are more sensitive to cellular structure and morphology; and during the process of cell death, during cancer treatment, dramatic changes in cell structure may give rise to a large ultrasound contrast between regions of responding and nonresponding cells.

It has been known since the late 1950s that ultrasound is sensitive to tissue changes that occur upon tissue degradation. Several investigators have examined the changes in ultrasound tissue properties during tissue decay (and presumably cell death). For example, in Carstensen's article [21] on the mechanisms of ultrasound absorption that was published in 1960, it is reported that Hueter [22] found that absorption in freshly excised tissue was approximately ten-times higher at 1 MHz than freshly excised liver (Figure 1). Conversely, Bamber *et al.* found that ultrasonic attenuation of mammalian organs is relatively insensitive to tissue degradation following excision (for up to 5 days), but ultrasound backscatter decreased after 24 h with the changes possibly beginning at the time of excision [23]. At clinical frequencies, Mimbs *et al.* found that a significant increase in integrated ultrasonic backscatter was correlated to cardiomyopathic changes caused by prolonged administration of doxorubicin [24]. Using much higher frequencies, O'Brien found that normal and infarcted myocardium differed in their properties; the attenuation coefficient of normal myocardium was significantly greater than that of infarcted myocardium and a significant increase in backscatter was observed [25]. Most of these early studies were focused at the tissue and organ level. The advent of high-frequency ultrasound later permitted the study of scattering from smaller cell ensembles. Sherar *et al.* found that ultrasound backscatter increased in the necrotic centers of spheroids (Figure 2) [26],

future medicine part of fsg

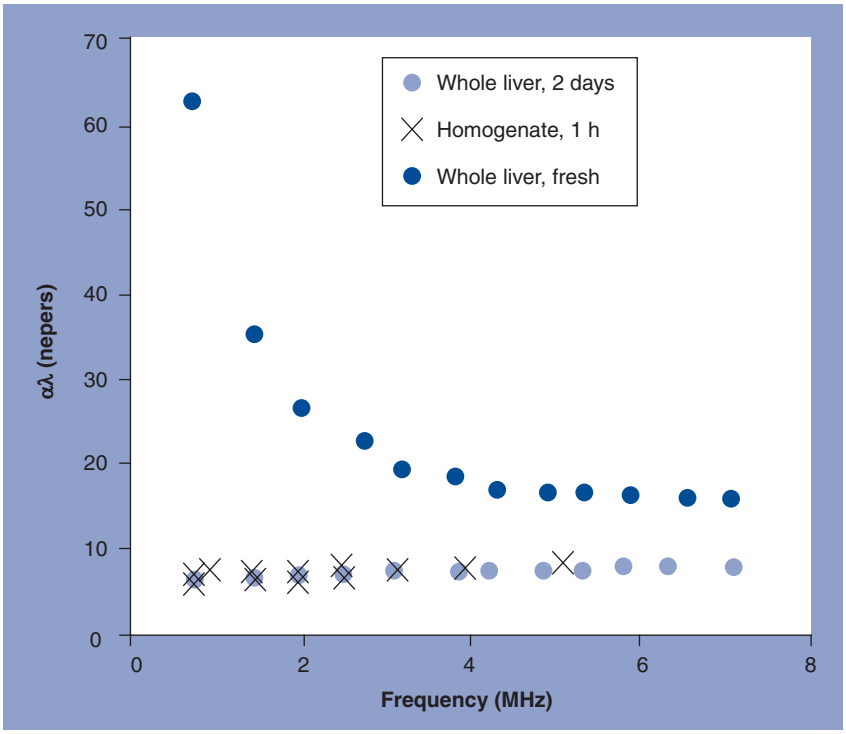

Figure 1. Absorption of sound as a function of frequency for fresh whole liver (dark gray), 'aged' for 2 days (light gray) and the same aged liver homogenized for 1 h (X). A significant drop of attenuation was measured following 2 days of liver 'aging'.
Adapted with permission from [21] © (1960) IEEE.

whereas Berube *et al.* expanded on these studies to look at the effects of nitromidazoles in mutlicellular spheroids [27]. This was the first work that indicated that high-frequency ultrasound, with wavelengths approaching the size of the cell, was sensitive to the structural changes that cells undergo during cell death and, unbeknown to the authors at the time, possibly apoptosis.

Quantitative ultrasound for cell death detection

The use of high-frequency (25–40 MHz) ultrasound to detect apoptotic cell death was first demonstrated by Czarnota and Kolios using a well-controlled system *in vitro* (Figure 3). In that study living cells, dead cells and cells that had died by programmed cell death or apoptosis were differentiated on the basis of their echogenicity. The study indicated increases in backscatter associated with different forms of cell death that were most prominent with apoptotic cell death. Leukemia cells treated with the chemotherapeutic drug cisplatinum undergoing apoptosis demonstrated a 16-fold increase in backscatter after 24 h of exposure in that study [28].

Further research has established the use of high-frequency ultrasound to detect cell death in tissues *ex vivo* and in live animals, and provided a potential morphological link explaining the associated imaging changes with further experimentation *in vitro.* Mouse brain tissue where apoptosis had been induced by photodynamic therapy (PDT) was imaged *ex vivo,* indicating spatially coincident increases in high-frequency ultrasound backscatter. Similarly, in skin, where apoptosis had been induced by PDT, comparable increases in ultrasound backscatter were demonstrated.

In vitro experiments that relied on drugs to induce nuclear condensation by arresting cells in the metaphase of mitosis (colchicine) have indicated a role for the condensation of the cell's nucleus in backscatter increases. Furthermore, subsequent enzymatic digestion of that condensed nuclear material using DNase results in a normalization of backscatter, further supporting a working hypothesis that nuclear configuration could alter backscatter from cells and tissues (Figure 3) [29]. Nuclear structure has subsequently been linked to backscatter properties in a high-frequency ultrasound examination of different cell types and their isolated nuclei in which speed of sound, attenuation coefficient and integrated backscatter coefficients were measured. Integrated backscatter coefficient values for cells and isolated nuclei showed much greater variation increasing from 1.71×10^{-4} Sr^{-1} mm^{-1} for the smallest nuclei to 26.47×10^{-4} Sr^{-1} mm^{-1} for cells with the largest nuclei. The findings have suggested that integrated backscatter coefficient values, but not attenuation or speed of sound, are correlated with the size of the nuclei [30].

Experiments with mixtures of apoptotic and viable cells have indicated further increases in backscatter compared with pure populations of apoptotic cells. This indicates a role for the effects of scatterer positions and their potential randomization towards contributing to increases in backscatter associated with cell death *in vivo* [31].

The application of spectral analysis methods to living and apoptotic cell samples *in vitro* have subsequently indicated the ability of classic tissue characterization methods to quantify the changes in acoustic properties associated with cell death in a number of experimental systems. Kolios *et al.* used calibrated backscatter spectra from regions-of-interest and linear regression techniques to calculate the spectral slope and midband fit of acoustic data obtained from various samples using 30–35 MHz ultrasound [32]. For apoptotic cells, the spectral slope increased from 0.37 dB/MHz before drug exposure to 0.57 dB/MHz 24 h after, corresponding to a change in effective scatterer radius from 8.7 to

3.2 µm. The midband fit increased in a time-dependent manner, peaking at 13 dB 24 h after cell death-inducing drug exposure. The statistical deviation of the spectral parameters was in close agreement with theoretical predictions [32–34].

Those same methods have also been applied to liver samples *ex vivo* where, in tissue models, ischemic cell death was linked to increases in backscatter ranging from 4 to 9 dBr and demonstrating kinetics dependent on tissue preservation conditions [35].

Apart from spectral methods, the use of signal envelope statistics to monitor and quantify structural changes during cell death have been investigated *in vitro* and *in vivo*. Signal envelope statistics have been examined by fitting to the Rayleigh and generalized Γ-distributions. The fit parameters of the generalized Γ-distribution have demonstrated sensitivity to structural changes in cells treated with chemotherapeutic drugs *in vitro*. The scale parameter demonstrated a 200% increase ($p < 0.05$) between untreated and cells treated for 24 h whereas the shape parameter showed a 50% increase ($p < 0.05$) over 24 h [31].

Cell death has also been detected *in vivo* using high-frequency ultrasound and spectral analysis methods in animal model systems where xenograft tumors were treated using a number of different methods. The first preclinical tumor-based use of high-frequency ultrasound spectroscopy was to noninvasively monitor tumor treatment by following xenograft malignant melanoma tumor responses to PDT *in vivo*. Banihashemi *et al.* observed a time-dependent increase in ultrasound backscatter variables after treatment. The observed increases in spectroscopic variables correlated with morphologic findings, indicating increases in apoptotic cell death, peaking at 24 h after PDT. Analyses of changes in spectral slope strongly correlated with changes in mean nuclear size over time, associated with apoptosis, after therapy [36]. Vlad *et al.* used high-frequency ultrasound in a similar manner to track the responses of xenograft tumors *in vivo* to radiotherapy. Data were collected with an ultrasound scanner using frequencies of 10–30 MHz. Ultrasound estimates calculated from normalized power spectra and parametric images (spatial maps of local estimates of ultrasound parameters) were used as indicators of response. Two of the mouse models (FaDu and C666-1) exhibited large hyperechoic regions at 24 h after radiotherapy. The ultrasound integrated backscatter increased by 6.5 to 8.2 dB ($p < 0.001$) and the spectral slopes increased from 0.77 to 0.90 dB/MHz for C666-1 tumors and from 0.54 to 0.78 dB/MHz for FaDu tumors ($p < 0.05$) in regions compared with preirradiated tumors. The hyperechoic regions in the ultrasound images corresponded in histology to areas of cell death. Parametric images were utilized in that study to further discern the tumor regions that responded to treatment [37].

Quantitative ultrasound & scattering physics

Conventional ultrasound images provide information regarding tissue echogenicity. Owing to the many instrument parameters that can be chosen during an imaging session, it is difficult to compare images between different ultrasound machines and even for the same machine when different settings are used. Quantitative ultrasound has been suggested as a method to overcome this limitation, since it uses metrics that are predominantly independent of the instrument settings to analyze the data (not to be confused with quantitative ultrasound narrowly defined to assess bone mineral density). A number of parameters that are based on

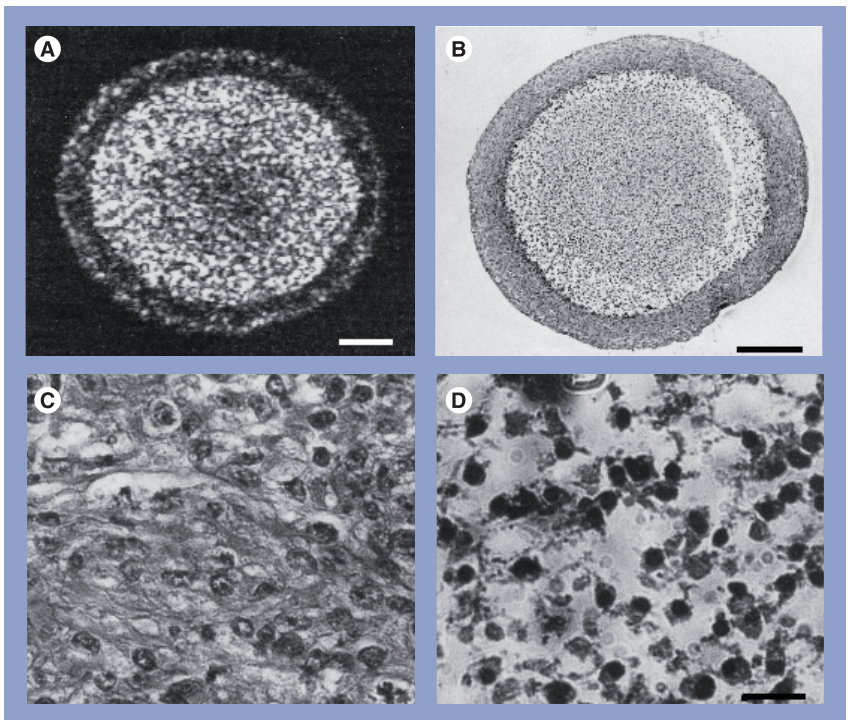

Figure 2. High-frequency tumor spheroid imaging demonstrating cellular morphology and related ultrasound contrast. (A) Shows a representative 100 MHz image of a tumor spheroid. **(B)** The appearance of an outer echo-poor rim and a more internal echogenic rim correlated with gross microscopic cross-section morphology of the spheroids. The scale bars indicate 500 µ. **(C)** Shows a higher magnification of the outer viable rim with intact cells. **(D)** Shows a representative section from a more internal rim corresponding spatially to the echogenic rim in the ultrasonograms. Note the appearance of cells with pyknotic nuclei corresponding to dying cells. The scale bar indicates 30 µ.
Images courtesy of FS Foster, University of Toronto, ON, Canada.

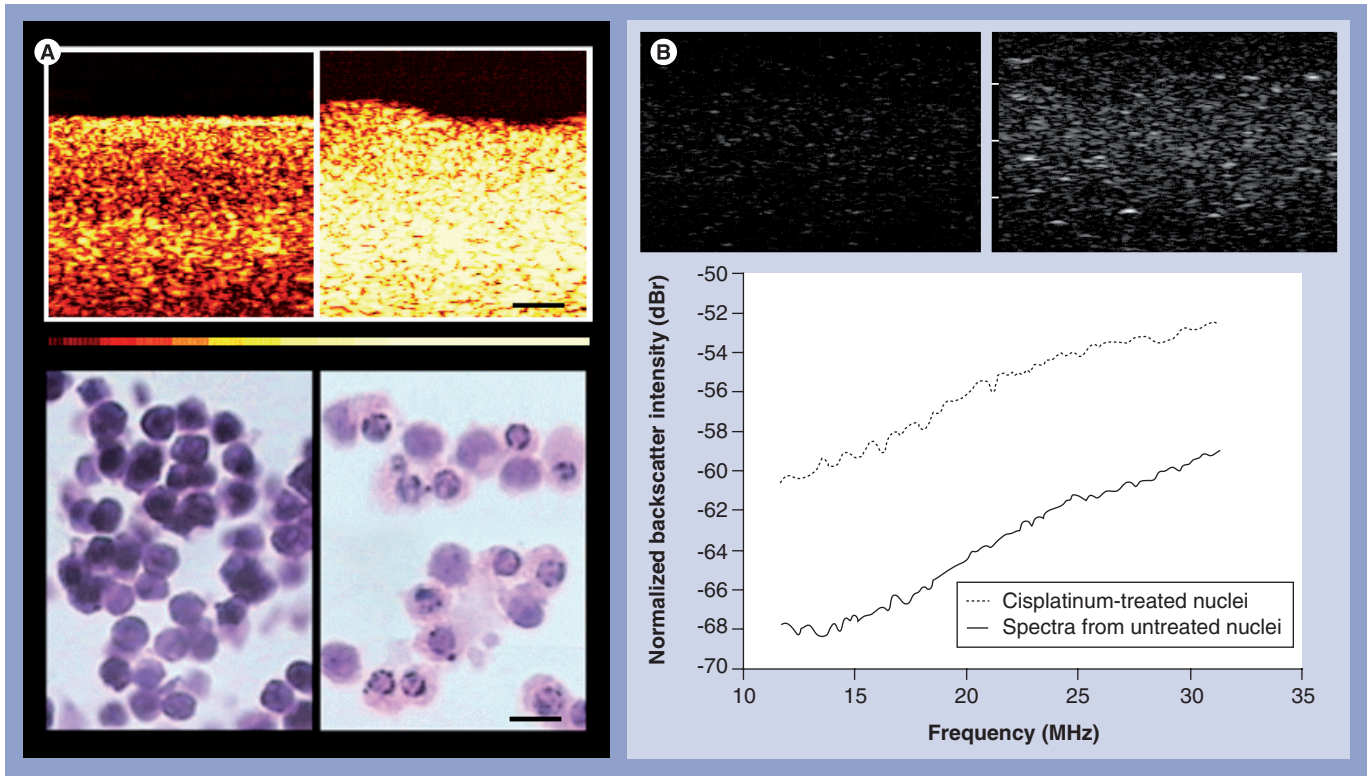

Figure 3. High-frequency ultrasound imaging of acute myeloid leukemia cells and their nuclei demonstrating the detection of cell death and the influence of nuclear morphology. (A) Top panels: ultrasound images (25 MHz) of acute myeloid leukemia (AML) cells after 0 h (left) and 24 h (right) of cisplatinum treatment. There is a mean increase of approximately 12 dB from left to right. The scale bar indicates 1 mm. Bottom panels: corresponding histology images of spreads of AML cells after 0 h (left) and 24 h (right) of cisplatinum treatment. Note the presence of condensed nuclear bodies beginning to marginate to the periphery of cells. The scale bar indicates 10 µ. **(B)** Ultrasound images (20 MHz) of AML nuclei in suspension before (left) and after (right) treatment with cisplatinum to induce apoptosis. Images are 8 mm wide. Note the increase in backscatter from the isolate apoptotic nuclei. The bottom panel indicates the difference in ultrasound spectra from the two samples of nuclei.

analyzing the backscatter radiofrequency (RF) echoes can be used: integrated backscatter, RF envelope statistics, frequency dependence of backscatter, ultrasound tissue attenuation, elastic properties of tissues, the propagation of shear waves in tissue and other more complex signal classification techniques such as entropy metrics of RF ultrasonic backscatter [38,39]. The majority of work in quantitative ultrasound that is based on the analysis of the backscatter patterns deal with tissue classification. Examples include the monitoring of changes in normal versus diseased livers [40,41], myocardial backscatter as a function of disease [42–44] and its variations during the cell cycle [45], and the discrimination of normal and cancerous tissue [46,47]. The use of quantitative ultrasound techniques for the detection of cell death is a relatively new development [32].

Our work has primarily focused on integrated backscatter, the frequency dependence of backscatter and the backscatter envelope statistics as a means to detect and potentially quantify cell death from anticancer therapies. We have found that high-frequency ultrasound (20–60 MHz) is particularly sensitive to the structural changes that cells and tissues undergo during treatment response [29,33] and we are currently investigating other frequency ranges. Most researchers are familiar with the improvements in ultrasound imaging capabilities at higher frequencies (namely better lateral and axial resolution), which come at the expense of penetration depth [48]. More subtle are the effects of the higher frequencies in terms of acoustical scattering physics and device contrast resolution, as it depends on the length scales involved in the particular application as well as the transducer characteristics [49]. Particularly important is the size of the scattering object compared with the ultrasound wavelength and the resolution cell of the ultrasound imaging instrument (defined as the volume of medium that contributes towards the signal at a particular instant of time). This volume is typically determined by the -6 dB lengths of the 'full width – half maximum' signal in the lateral dimension and the -6 dB pulse length in the axial dimension. As the frequency increases, these parameters give rise to variations in the

population of scatterers that contribute to the ultrasound signal and therefore the contrast resolution. One example is the scattering from blood. In the clinical low-frequency ultrasound imaging range, blood vessels appear as black cylinders of low echogenicity since the scattering strength of red blood cells is very low compared with the surrounding tissue. However, at higher frequencies, the scattering from the red blood cells is comparable to that of the surrounding tissue; in some cases the signal from the blood is stronger than that of the surrounding tissues [50]. Moreover, there can be large variations in the backscatter depending on whether the red blood cells are enucleated or not [50].

The relationship between the ultrasound wavelength and the scatterer size is typically expressed as the product of the wavenumber k and the scatterer size a. When the ultrasound wavelength is much smaller than the scattering structure size ($ka >> 1$), then the well-known simple equations of reflection and refraction can be used to study ultrasound scattering. This is also known as class 3 scattering and is typically specular in nature [51,52]. An example of class 3 scattering is the interface between organs. When the ultrasound wavelength is much larger than the scattering structure size ($ka << 1$), then several approximations can be made to the solution of a pressure wave incident on an object (this is the Rayleigh scattering regime – the scattering intensity increases with the fourth power of frequency and sixth power of the scatterer radius). In this case the concentration of scatterers per resolution cell is typically high and the images produced have the typical speckle pattern seen in ultrasound images. This is also known as class 1 scattering [51,52]. When the ultrasound wavelength approaches the size of the scattering structure ($ka \cong 1$), then the full equations of a traveling pressure wave incident on a scattering structure have to be solved [53]. Approximations can still be made since tissue scattering is typically weak (e.g., the Born approximation) [54,55]; however, the problem still remains difficult to solve for tissues. Class 2 scattering occurs when the scattering structure has concentrations lower than 1 per resolution cell; these scatterers cause scattering patterns that can be differentiated from the speckle that is produced in class 1 scattering. In both class 1 and 2 scattering there is a frequency dependence of the scattering that can be used to infer the dimensions of the scattering structure [56,57].

In the study of frequency dependence of the ultrasound scattering it is important to note that that increasing the frequency of the interrogating ultrasound improves not only spatial resolution, but it also changes the nature of the dominant ultrasonic scattering structures. As $ka \approx 1$ then the new structures that meet this criterion start to contribute more to the backscattered ultrasound signal detected by the transducers and thus the frequency dependence of the backscatter [49,58]. Therefore, the contrast resolution also changes with frequency.

We have hypothesized that for the frequencies of interest (20–60 MHz), the cell's nucleus is a major contributor to the ultrasound backscatter [30]. In the case of cancer treatment monitoring, as the cell and nucleus structure are of the greatest importance in the determining responses to interventions, scattering falls within the regime of class 1 or 2 scattering for clinical and high-frequency ultrasound (1–60 MHz). The ultrasound wavelengths for these frequencies range from 1.5 mm down to 25 µm. As a result, tumors with a large concentration of cells (with diameters ranging from 10 to 30 µm) typically result in a speckle pattern in the ultrasound images. Speckle arises when there are many unresolved scatterers of similar scattering strength per resolution volume of the imaging device [59–61]. Speckle is often referred to as 'speckle noise' because it can interfere with the delineation of boundaries between two media (class 1 scattering). However, speckle is deterministic in the sense that for a given spatial distribution of scatterers the speckle pattern remains the same and does not vary in time. Therefore, it is not noise in the conventional sense; in fact, for the high-frequency imaging of cells in which individual cells cannot be resolved, the entire content of the image is speckle (Figure 3A) [31].

We have focused our effort on the analysis of ultrasound RF: the frequency dependence and the envelope statistics of the RF data. In this case spectrum and statistical analyses of RF data may be used to infer scatterer properties as these can be theoretically linked to scatterer sizes and concentrations within biological samples. Whereas biological samples may exhibit features with stochastically influenced distribution of acoustic scatterer sizes and concentrations, RF analysis of ultrasound data as per Lizzi *et al.* [13] may be used to provide information regarding these scatterer sizes and concentrations.

The biology of cell death

Cell death and its specialized morphological forms (apoptosis, oncolysis, mitotic arrest and necrosis) have been studied as far back as 1842 with the first morphological descriptions being made shortly thereafter [62]. These forms of cell

death are morphologically different, although they do share certain common features. Their unique morphological features are associated with potentially different viscoelastic properties, leading to differences in acoustic properties that permit their detection and potential differentiation using ultrasound. For the purposes of discussion here we refer to necrosis as the end state of all of these cell death forms.

Apoptosis is a specialized form of death that is genetically programmed with unique morphological features that differentiate it from other forms of cell death. It is genetically controlled and induced in certain developmental stages, homeostatic processes and in response to a wide variety of cancer therapies. With this mode of cell death, a characteristic aggregation of chromatin occurs forming a pyknotic nucleus that then breaks down into visible macroscopic fragments. These fragments then marginate at the periphery of the nucleus and after dissolution of the nuclear membrane, further translocate to the edge of the cell. The cell's DNA during this process begins to be specifically enzymatically digested, resulting in further changes to the cell's nuclear material. In addition, the cellular membrane during this process begins to change morphology becoming blebbed and, ultimately, the cell breaks down with its cellular components compartmentalized within vesicles [62].

Oncotic cell death refers to accidental cell death accompanied by cellular swelling, organelle swelling, blebbing and increased membrane permeability. This mechanism is based on failure of the ionic pumps of the plasma membrane. This type of death is typically caused by ischemia and possibly by toxic agents that interfere with ATP generation or increases in the permeability of the plasma membrane. The DNA in this form of cell death breaks down in a nonspecific manner in contrast to apoptosis, and is accompanied by organelle swelling and vacuolization, protein denaturation and hydrolysis. Large blebs of cellular contents may burst in this process, resulting in inflammatory changes. The process may be associated with karyorrhexis (nuclear fragmentation) and is associated with karyolysis (the complete dissolution of the chromatin matter due to the activity of DNase). The word necrosis is often substituted for oncotic cell death, although necrosis more accurately refers to dead cells regardless of the particular cell death pathway involved in the induction of death.

In mitotic death cells may arrest at the G2/M checkpoint with canonically condensed chromosomes in the form of mitotic bodies and an absence of a nuclear membrane. These cells have a unique morphology in that they may accumulate aneuploid complements of nuclear material and present with multiple nuclei. They may be considered dead in the functional sense that they cannot reproduce by cell division. Attempts at cellular division lead to death by either apoptosis or a nonapoptotic cell death depending on various circumstances.

There remains limited information on the biophysical properties of these forms of cell death since only now are methods being established to measure viscoelastic properties of biomaterials at a cellular level. Quartz crystal microbalance biosensor techniques have been used to study responses of apoptotic mammary epithelial tumor cells to taxanes. This method measures mass coupling and viscoelastic properties of the cells associated with the crystal surface, which can be measured continuously and are based on shifts in crystal f and motional R values, and showed that these change with cell death [63]. Other studies have used cell deformation techniques to measure cell cortical tension and cellular viscosity. In those studies, colchicine and paclitaxel, which induce mitotic arrest after nuclear condensation, caused disruption of microtubular structures, but had little effect on either F-actin or on cellular mechanical properties except at higher concentrations where it caused increased actin polymerization and increases in cell rigidity. In addition, there were increases in the characteristic cellular viscosity by 30–50%, increases in the dependence of viscosity on shear rate by 10–20% and the cortical tension by 18–21% [64]. Morphology changes in cells undergoing apoptosis are also expected to result in changes in cellular elasticity and viscosity that potentially result in acoustic property changes. Microrheological methods [65–67] are one manner in which such changes can be assessed. Estimates that have been made using PC3 prostate cells exposed to 1 µg/ml cisplatinum, which induces apoptotic cell death, indicate that after 9–12 h of exposure concomitant with nuclear condensation and the onset of fragmentation, the elastic and viscous moduli increased by over 50 and 20 Pa, respectively, over the course of the treatment [68].

Ultrasound backscatter & cell death

The main ultrasound changes responsible for the ultrasound detection of apoptosis are related to the scattering intensity and its frequency dependence, as described in the previous section. Early stages of cell death generally lead to large

increases (6–12 dB) in ultrasound backscatter intensity for both cell aggregate [28,31,33] and preclinical [36,37] models. For advanced stages of cell death, the backscatter intensity decreases [69]. The spectral slope, which is a measure of the frequency dependence of the scattered ultrasound, has been found to increase in cell samples and *in vivo* with tumor responses for which the predominant mode of cell death appeared to be apoptosis [32,36]. By contrast, the spectral slope has remained relatively constant with samples in which there was a mixture of cell death modes, and has decreased in samples that predominantly underwent mitotic arrest/catastrophe [33]. Another striking feature of the recent *in vivo* experiments is that tumor responses, as assessed both by histology and ultrasound, have shown excellent spatial correspondence, both indicating sharp gradients between responding and non-responding regions. Moreover, the magnitude of the *in vivo* spectral parameter changes that have been measured ultrasonically are similar to the changes measured with *in vitro* experimental systems we have developed [70]. Even though tumor tissues are complex structures consisting of cells of different sizes and different composition that are intermixed with blood vessels and lymphatics, similar values of ultrasound integrated backscatter were measured from cell samples and tumor xenografts originated using the same cell line. This has suggested that the tumor cells in the *in vivo* tumor dominate the contribution to the backscattered ultrasound [70].

It is difficult to conclusively ascertain the origin of the scattering increase and spectral changes observed in the model systems. With apoptosis and cell death in general, we hypothesize that the changes in the cell structure and composition (e.g., cell swelling, nuclear condensation and fragmentation, and chromatin dissolution) create spatial and temporal changes in the scattering structures that permit the detection of regions of cell death for a range of frequencies that are used in clinical and preclinical imaging. In the range of 20 to 60 MHz (ultrasound wavelengths of 75 and 25 µm, respectively) the ka values range from 0.8 to 2.5 (for a cell of 10 µm diameter) and 2.5 to 7.5 (for a cell of 30 µm diameter) and therefore lie in the regime for which ultrasound is sensitive to changes in structure. Since our work to date has indicated that the nucleus is the main scattering source in highly cellular tumors, these represent the upper bound of ranges owing to the smaller nucleus size. Moreover, a series of experiments designed to elucidate the changes in ultrasound backscatter characteristics seem to correlate to changes in the nuclear structure. Therefore, changes in the backscattering characteristics can be used to probe changes in gross nuclear structure (e.g., those that occur during cell death – oncolysis and apoptosis) or for the classification of tumors (enlarged cell nuclei are a prime indicator of cell malignancy).

Other modalities for cell death detection

A number of other imaging-based methods have recently been developed that can detect cell death in tumor responses to treatment, as reviewed in Brindle [71]. These include 2-^{18}F-fluoro-2-deoxy-D-glucose PET and ^{13}C-hyperpolarized pyruvate imaging as markers of tumor glucose metabolism, 3′-deoxy-3′-^{18}F flurothymidine for DNA synthesis, and PET and magnetic resonance spectroscopy for amino acid and lipid metabolism. Furthermore, early tumor cell death during treatment is now recognized to be a good prognostic indicator of outcome [71] and can be detected using magnetic resonance techniques and antibody-based labeling imaging using SPECT, PET, MRI and optical imaging. In addition, MRI has been used to study apoptosis on the basis that cells dying by this process undergo modifications in water content. Most studies published have relied on gadolinium to probe water content changes [72,73]. *In vivo*, any primary signal changes associated with apoptotic cells in tissue parenchyma would be potentially convoluted with signal changes caused by differences in vascular permeability to gadolinium, which may occur with vascular cell death. Specific approaches have relied on gadolinium chelates of the C2A domain of synaptotagmin-I, which binds to phosphatidyl serine exposed on apoptotic and apo-necrotic cell membranes [74]. Other new approaches have relied on measurements of intracellular sodium with MRI and have found this to correlate with taxotere chemosensitivity-induced regions of apoptosis [75]. Studies have demonstrated the further utility of T1rho and T2rho MRI for apoptosis detection [76]. However, compared with these imaging modalities, ultrasound has the advantage that endogenous contrast is used to evaluate treatment effectiveness, without the need of injection of any contrast agents or molecular markers; the contrast is generated by the very process of cell death itself.

Conclusion

Quantitative ultrasound methods can be used to characterize cell death changes in cells, tissues and tumors. In principle these changes

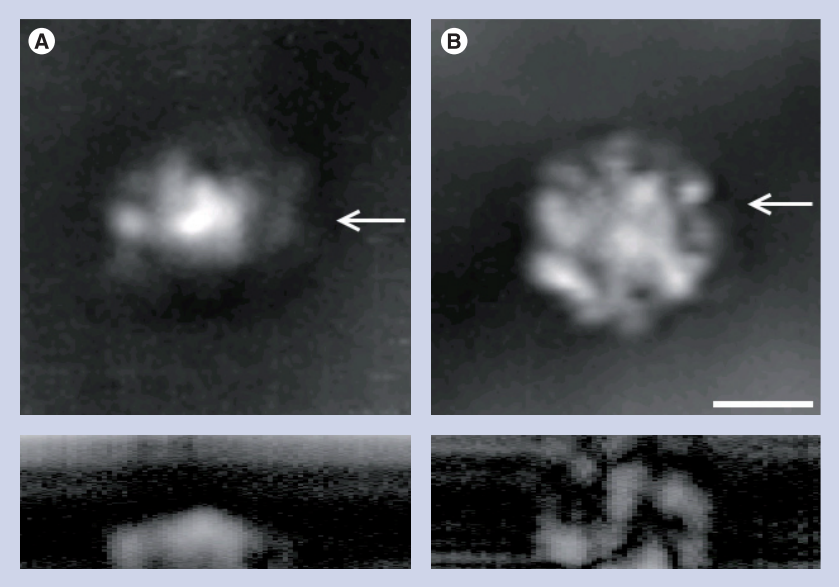

Figure 4. Very high-frequency ultrasound microscopy of cells undergoing apoptotic death. A comparison of the backscatter signal from **(A)** an unresponsive MCF-7 breast cancer cell and **(B)** a responsive cell undergoing apoptosis after paclitaxel chemotherapy treatment acquired with a 375-MHz transducer. The c-scan backscatter image is shown on top, and the b-scan showing the scattering regions from the cell is on the bottom. The location of the b-scan plane is indicated by the arrow. Before apoptosis the backscatter signal originates primarily from the region close to the cell nucleus, whereas after the cell response scattering regions appear throughout the entire cell. The scale bar indicates 15 µ.

result in cell morphology changes leading to consequent changes in the acoustical properties of these cells, which in turn permits their detection with high-frequency ultrasound. The advantage of this methodology is that it is non-invasive, does not require contrast agents, does not rely on radioactive agents and compared with other imaging modalities remains inexpensive, portable and images can be produced rapidly. A limitation of high-frequency ultrasound is that when interacting with cells and tissues there is a limited penetration depth of only several centimeters due to tissue attenuation. In terms of the scattering of high-frequency ultrasound, owing to the ratio of the scattering structures (cells and nuclei) to the interrogating frequency (with a wavelength similar in size to cells and nuclei) the modeling of the physical process of scattering remains complex. However, there are emerging developments in ultrasound that address both of these issues. Recent developments that permit the facile collection of RF data with clinical-frequency range ultrasound devices are now enabling the use of low-frequency ultrasound to detect cell death. In terms of better understanding the physics of ultrasound backscatter at a single cell or nucleus level, recently developed very high-frequency ultrasound microscopes can be used with live cells or isolated nuclei while maintaining them in physiological conditions during studies. These developments are leading towards a clinical implementation of cell death detection and a better understanding of the physics behind the detection of cell death using ultrasound.

Future perspective

■ Very high-frequency ultrasound & cell death

Key to the understanding of the changes in ultrasound backscatter are the mechanical characteristics of cells, and how these characteristics change during cell death. In order to determine these characteristics at the length scale of interest (microns), low- and high-frequency ultrasound cannot be used, as the measurement resolution is too coarse. To this end, microrheology techniques have been developed to probe the mechanical properties of cells and cell cultures. Using such techniques, it has been demonstrated that at high frequencies, the cell nucleus was more stiff than the cytoplasm [77]; the nucleus was more rigid at high rates of deformation and more liquid-like at low deformation rates, with a viscoelastic modulus at least two-times greater than that of the cytoplasm. This suggests that the nucleus is a potential scattering source, consistent with our hypothesis. Moreover, our recent experiments indicate an increase of the cell elasticity (spring-like nature) with treatment [68]. Even though these measurements have been made at low frequencies of greater relevance to ultrasound shear wave imaging, our group is working on expanding the relevant ranges to include kHz and potentially MHz measurements.

Another approach has involved the use of acoustic microscopy to elucidate cellular ultrasonic and mechanical properties. At 1 GHz, the wavelength of ultrasound is close to 1.5 µm, and therefore a comparable spatial resolution can be achieved. Bulk measurements of ultrasound attenuation have shown an increase in the ultrasound attenuation for cells undergoing apoptosis [78,79] and large temporal changes in ultrasound backscatter as a function of time after response to chemotherapy exposure [79]. Even though these measurements are performed at very high frequencies, and therefore findings related to ultrasonic backscatter may not have direct relevance to the lower frequency ranges (since different scattering structures meet the $ka \approx 1$ criterion), analysis of the scattering patterns can provide insight into the process of

ultrasonic scattering. The attenuation coefficient (in dB/cm/MHz) and speed of sound are not expected to vary substantially at these higher frequencies since these parameters are mainly determined by the molecular composition of the cells and not structure. However, parameters such as the scattering coefficient and shear modulus are related to features of higher structural levels, and therefore can be expected to exhibit greater variation for different frequencies of interrogation [80]. Once the properties of the individual cells have been elucidated, one can construct theoretical models to model the scattering process [53,81]. This, however, is complicated by the fact that, irrespective of the acoustical properties of the individual scatterers, the spatial distribution of the scattering sources on their own is a source of large variation in ultrasound backscatter [82,83]. Separating the individual contributions of changes of scattering properties from the effects of any changes in scatter spatial distribution to the changes of ultrasound backscattered detected has proven to be a difficult task and is an area of intense research activity in our laboratories.

Very high-frequency ultrasound (100 MHz to 2 GHz) has been used previously to study primarily inorganic substances and excised tissues *ex vivo*. Recent developments that permit the confocal light and ultrasound microscopy of living cells while growing in culture have spurred a resurgence in the field. It is now possible to investigate the acoustical properties of living cells as well as cells dying through specific cell death pathways. As an example, we have used 100 MHz to 1 GHz ultrasound to study apoptosis and demonstrated that at 400 MHz subcellular changes in backscatter appear to be associated with regions of nuclear material aggregation that occurs during apoptosis (Figure 4). At high frequencies (1 GHz) other factors seem to potentially predominate in the formation of backscatter images.

■ Conventional frequency ultrasound of cell death

Conventional (low) to mid-range ultrasound frequencies (1–20 MHz) are applicable clinically and have been used in medicine since the development of ultrasound technology. The detection of tissue changes related to cell death in the case of necrosis dates back nearly 50 years with decreases in backscatter being observed. Nevertheless, it is only now, that methods in quantitative ultrasound are being applied at clinically relative frequencies for cell death detection. We have recently applied the use of 7-MHz ultrasound (3–10 MHz -6 dB

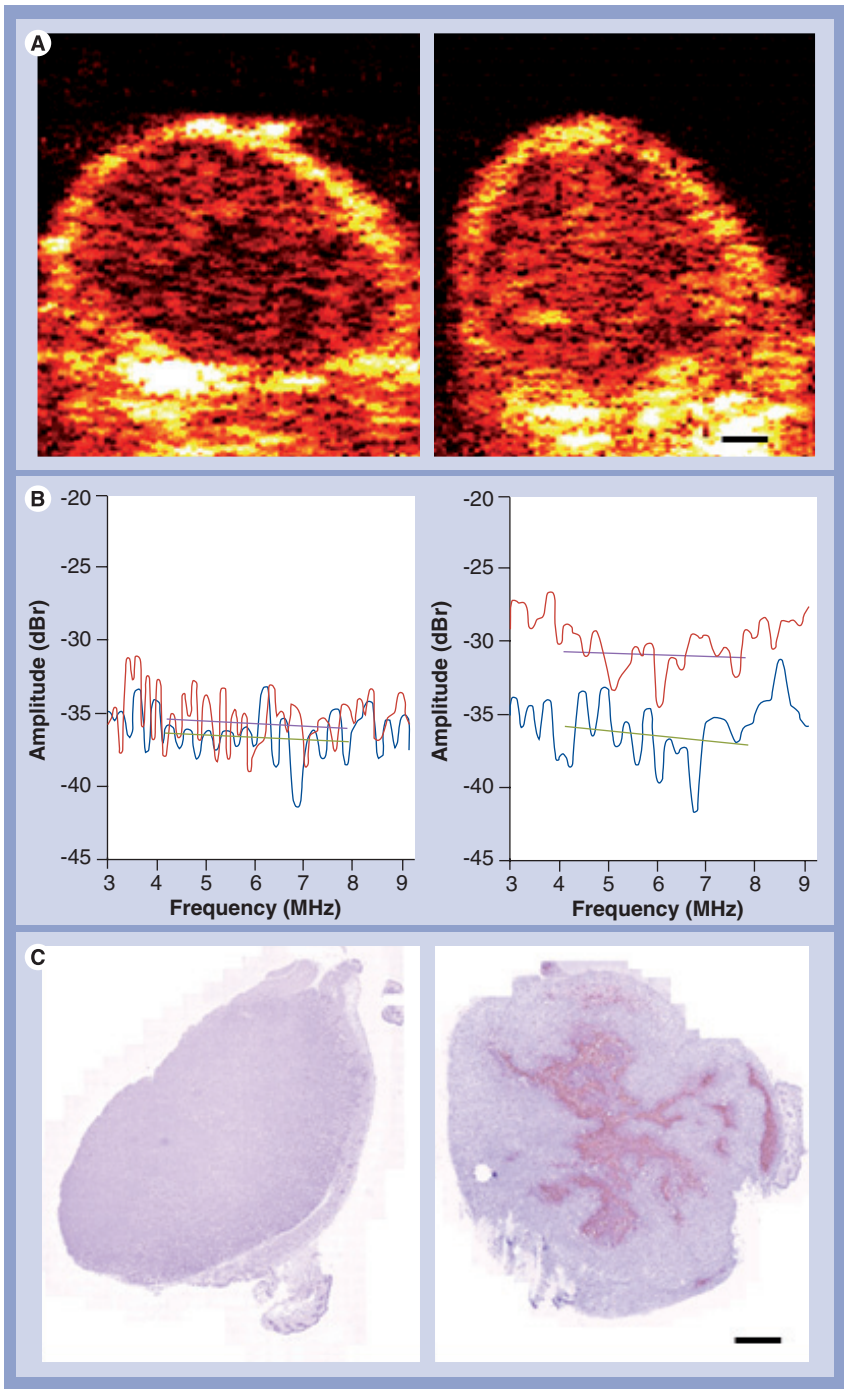

Figure 5. Conventional frequency ultrasound and cell death detection. **(A)** Conventional 7 MHz frequency ultrasonograms of representative PC3 prostate tumors after a novel microbubble-based antivascular therapy. The left tumor is a representative untreated tumor whereas the one on the right is a tumor after treatment. The scale bar indicates 1 mm. The increase is consistent with 6 dBr. The fitted line is a linear best fit over the -6 dB bandwidth of the transducer. **(B)** Associated normalized backscatter spectra from tumors before (green) and after (red) treatment. The control animal received sham treatment. **(C)** Representative terminal deoxynucleotidyl transferase dUTP nick end labeling (TUNEL) histology for untreated and treated tumors (left and right, respectively). The treated tumor demonstrates significant cell death. The scale bar indicates 1 mm.

bandwidth) to the detection of cell death using acute myeloid leukemia cells *in vitro* and tumors treated with radiation with or without anti-angiogenics in combination. Data from experiments with cells have demonstrated an ability to detect as little as 10% apoptotic cells with data paralleling changes observed using high-frequency ultrasound. Moreover, ultrasound data detected from prostate cancer PC3 tumor xenografts, where anti-angiogenic agents were used in combination with radiation to induce large macroscopic areas of cell death, indicate that the detection of apoptosis may also be carried out *in vivo*. These emerging results (Figure 5) suggest that the monitoring of treatment efficacy may be possible using low-frequency ultrasound and such evaluations are underway in patients receiving cancer therapy.

Acknowledgements

We thank E Strohm and N Papanicolau for assistance with figures. We thank A Giles and A Worthington for many years of dedicated assistance with experiments.

Financial & competing interests disclosure

MC Kolios holds a Tier 2 Canada Research Chair in Biomedical Applications of Ultrasound. GJ Czarnota holds a Cancer Care Ontario Research Chair in Experimental Therapeutics and Imaging. The research here was supported by grants from the Natural Sciences and Engineering Council of Canada and the Canadian Institutes of Health Research to both GJ Czarnota and MC Kolios, and infrastructure grants from the Canadian Foundation of Innovation, Ontario Ministry of Research and Innovation and Ryerson University. MC Kolios and GJ Czarnota are authors on an issued patent ('Detection of Apoptosis Using High- Frequency Ultrasound' US patent #6511430) and a pending patent ('Methods of monitoring cellular death using low frequency ultrasound' US patent application #11/455,005) held by the University Health Network (Toronto, Ontario, Canada) and licensed to VisualSonics, Inc. (Toronto, ON, Canada). The authors have no other relevant affiliations or financial involvement with any organization or entity with a financial interest in or financial conflict with the subject matter or materials discussed in the manuscript apart from those disclosed.

No writing assistance was utilized in the production of this manuscript.

Executive summary

- We have been developing methods to detect cell death using high-frequency ultrasound and quantitative ultrasound methods.
- The applicability of such methods for cell death detection has been demonstrated *in vitro* and *in vivo* using a number of model tumor types and cell death-inducing treatments.
- The scattering process of ultrasound from single cells is now being evaluated from ultrasound microscopy research.
- The quantitative ultrasound methods used for cell death detection are now also being extended to clinical frequency ranges and are being evaluated in patients to monitor the efficacy of cancer therapies.
- These methods provide a potential manner of evaluating and monitoring the efficacy of cancer therapies in the future.

Bibliography

Papers of special note have been highlighted as:
▪ of interest
▪▪ of considerable interest

1 Forsberg F: Ultrasonic biomedical technology; marketing versus clinical reality. *Ultrasonics* 42(1), 17–27 (2003).

2 Goldberg BB, Liu JB, Forsberg F: Ultrasound contrast agents: a review. *Ultrasound Med. Biol.* 20(4), 319–333 (1994).

3 Forsberg F, Merton DA, Liu JB, Needleman L, Goldberg BB: Clinical applications of ultrasound contrast agents. *Ultrasonics* 36(1–5), 695–701 (1998).

4 Kaufmann BB, Lindner JR: Molecular imaging with targeted contrast ultrasound. *Curr. Opin. Biotechnol.* 18(1), 11–16 (2007).

5 Ophir J, Alam SK, Garra B *et al.*: Elastography: ultrasonic estimation and imaging of the elastic properties of tissues. *Proc. Inst. Mech. Eng.* 213(3), 203–233 (1999).

6 Garra BS: Imaging and estimation of tissue elasticity by ultrasound. *Ultrasound Q.* 23(4), 255–268 (2007).

7 Dahl JJ, Dumont DM, Allen JD, Miller EM, Trahey GE: Acoustic radiation force impulse imaging for noninvasive characterization of carotid artery atherosclerotic plaques: a feasibility study. *Ultrasound Med. Biol.* 35(5), 707–716 (2009).

8 Zhai L, Palmeri ML, Bouchard RR, Nightingale RW, Nightingale KR: An integrated indenter-arfi imaging system for tissue stiffness quantification. *Ultrason. Imaging* 30(2), 95–111 (2008).

9 Chen S, Urban MW, Pislaru C *et al.*: Shearwave dispersion ultrasound vibrometry (SDUV) for measuring tissue elasticity and viscosity. *IEEE Trans. Ultrason. Ferroelectr. Freq. Control* 56(1), 55–62 (2009).

10 Muller M, Gennisson JL, Deffieux T, Tanter M, Fink M: Quantitative viscoelasticity mapping of human liver using supersonic shear imaging: preliminary *in vivo* feasibility study. *Ultrasound Med. Biol.* 35(2), 219–229 (2009).

11 Chivers RC, Hill CR: A spectral approach to ultrasonic scattering from human tissue: methods, objectives and backscattering measurements. *Phys. Med. Biol.* 20(3), 799–815 (1975).

12 Cohen RD, Mottley JG, Miller JG, Kurnik PB, Sobel BE: Detection of ischemic myocardium *in vivo* through the chest wall by quantitative ultrasonic tissue characterization. *Am. J. Cardiol.* 50(4), 838–843 (1982).

13 Lizzi FL, Greenebaum M, Feleppa EJ, Elbaum M, Coleman DJ: Theoretical framework for spectrum analysis in ultrasonic tissue characterization. *J. Acoust. Soc. Am.* 73(4), 1366–1373 (1983).

▪▪ **Theoretical framework is described in this research paper, which forms the basis for quantitative ultrasound as used in current applications.**

14 Coleman DJ, Lizzi FL: Computerized ultrasonic tissue characterization of ocular tumors. *Am. J. Ophthalmol.* 96(2), 165–75 (1983).

15 Shung KK: Ultrasonic characterization of biological tissues. *J. Biomech. Eng.* 107(4), 309–314 (1985).

16 Silverman RH, Coleman DJ, Lizzi FL *et al.*: Ultrasonic tissue characterization and histopathology in tumor xenografts following ultrasonically induced hyperthermia. *Ultrasound Med. Biol.* 12(8), 639–645 (1986).

17 Feleppa EJ, Lizzi FL, Coleman DJ, Yaremko MM: Diagnostic spectrum analysis in ophthalmology: a physical perspective. *Ultrasound Med. Biol.* 12(8), 623–631 (1986).

18 Lizzi FL, Ostromogilsky M, Feleppa EJ, Rorke MC, Yaremko MM: Relationship of ultrasonic spectral parameters to features of tissue microstructure. *IEEE Trans. Ultrason. Ferroelectr. Freq. Control* 34(3), 319–329 (1987).

19 Lizzi FL, King DL, Rorke MC *et al.*: Comparison of theoretical scattering results and ultrasonic data from clinical liver examinations. *Ultrasound Med. Biol.* 114(5), 377–385 (1988).

20 Lizzi FL, Astor M, Feleppa EJ, Shao M, Kalisz A: Statistical framework for ultrasonic spectral parameter imaging. *Ultrasound Med. Biol.* 23(9), 1371–1382 (1997).

21 Carstensen EL: The mechanism of the absorption of ultrasound in biological materials. *IRE Trans. Med. Electron.* ME-7, 158–162 (1960).

22 Hueter TF: Visco-elastic losses in tissues in the ultrasonic range. Wright Air Dev Center, Wright-Patterson Air Force Base, Tech. Rept. No 57-106, ASTIA Doc No. AD142171; August (1958).

23 Bamber JC, Fry MJ, Hill CR, Dunn F: Ultrasonic attenuation and backscattering by mammalian organs as a function of time after excision. *Ultrasound Med. Biol.* 3(1), 15–20 (1977).

24 Mimbs JW, O'Donnell M, Miller JG, Sobel BE: Detection of cardiomyopathic changes induced by doxorubicin based on quantitative analysis of ultrasonic backscatter. *Am. J. Cardiol.* 47(5), 1056–1060 (1981).

25 O'Brien PD, O'Brien WD Jr, Rhyne TL, Warltier DC, Sagar KB: Relation of ultrasonic backscatter and acoustic propagation properties to myofibrillar length and myocardial thickness. *Circulation* 91(1), 171–175 (1995).

26 Sherar MD, Noss MB, Foster FS: Ultrasound backscatter microscopy images the internal structure of living tumor spheroids. *Nature* 330(6147), 493–495 (1987).

▪ **Presents data showing the contrast differences between living and dead regions of cell spheroids.**

27 Berube LR, Harasiewicz K, Foster FS, Dobrowsky E, Sherar MD, Rauth AM: Use of a high frequency ultrasound microscope to image the action of 2-nitroimidazoles in multicellular spheroids. *Br. J. Cancer* 65(5), 633–640 (1992).

28 Czarnota GJ, Kolios MC, Vaziri H *et al.*: Ultrasonic biomicroscopy of viable, dead and apoptotic cells. *Ultrasound Med. Biol.* 23(6), 961–965 (1997).

29 Czarnota GJ, Kolios MC, Abraham J *et al.*: Ultrasound imaging of apoptosis: high-resolution non-invasive monitoring of programmed cell death *in vitro*, *in situ* and *in vivo*. *Br. J. Cancer* 81(3), 520–527 (1999).

▪▪ **Presents the first data on the specific ultrasound imaging of apoptotis *in vitro, in situ* and *in vivo*.**

30 Taggart LR, Baddour RE, Giles A, Czarnota GJ, Kolios MC: Ultrasonic characterization of whole cells and isolated nuclei. *Ultrasound Med. Biol.* 33(3), 389–401 (2007).

▪▪ **Provides strong experimental evidence that supports the hypothesis that the nucleus is the dominant scattering structure in cell aggregates.**

31 Tunis AS, Czarnota GJ, Giles A, Sherar MD, Hunt JW, Kolios MC: Monitoring structural changes in cells with high frequency ultrasound signal statistics. *Ultrasound Med. Biol.* 31(8), 1041–1049 (2005).

32 Kolios MC, Czarnota GJ, Lee M, Hunt JW, Sherar MD: Ultrasonic spectral parameter characterization of apoptosis. *Ultrasound Med. Biol.* 28(5), 589–597 (2002).

33 Vlad RM, Alajez NM, Giles A, Kolios MC, Czarnota GJ: Quantitative ultrasound characterization of cancer radiotherapy effects *in vitro*. *Int. J. Radiat. Oncol. Biol. Phys.* 72(4), 1236–1243 (2008).

34 Brand S, Solanki B, Foster DB, Czarnota GJ, Kolios MC: Monitoring of cell death in epithelial cells using high frequency ultrasound spectroscopy. *Ultrasound Med. Biol.* 35(3), 482–493 (2009).

35 Vlad RM, Czarnota GJ, Giles A, Sherar MD, Hunt JW, Kolios MC: High-frequency ultrasound for monitoring changes in liver tissue during preservation. *Phys. Med. Biol.* 50(2), 197–213 (2005).

36 Banihashemi B, Vlad R, Debeljevic B, Giles A, Kolios MC, Czarnota GJ: Ultrasound imaging of apoptosis in tumor response: novel preclinical monitoring of photodynamic therapy effects. *Cancer Res.* 68(20), 8590–8596 (2008).

▪▪ **Presents the first use of quantitative high-frequency ultrasound to monitor cell death effects in tumors in response to anticancer treatments *in vivo*.**

37 Vlad RM, Brand S, Giles A, Kolios MC, Czarnota GJ: Quantitative ultrasound characterization of responses to radiotherapy in cancer mouse models. *Clin. Cancer Res.* 15(6), 2067–2075 (2009).

38 Hughes MS, Marsh JN, Zhang H *et al.*: Characterization of digital waveforms using thermodynamic analogs: detection of contrast-targeted tissue *in vivo*. *IEEE Trans. Ultrason. Ferroelectr. Freq. Control* 53(9), 1609–1616 (2006).

39 Wallace KD, Marsh JN, Baldwin SL *et al.*: Sensitive ultrasonic delineation of steroid treatment in living dystrophic mice with energy-based and entropy-based radiofrequency signal processing. *IEEE Trans. Ultrason. Ferroelectr. Freq. Control* 54(11), 2291–2299 (2007).

40 Guimond A, Teletin M, Garo E *et al.*: Quantitative ultrasonic tissue characterization as a new tool for continuous monitoring of chronic liver remodeling in mice. *Liver Int.* 27(6), 854–864 (2007).

41 Yang M, Krueger TM, Miller JG, Holland MR: Characterization of anisotropic myocardial backscatter using spectral slope, intercept and midband fit parameters. *Ultrason. Imaging* 29(2), 122–134 (2007).

42 Vered Z, Barzilai B, Mohr GA *et al.*: Quantitative ultrasonic tissue characterization with real-time integrated backscatter imaging in normal human subjects and in patients with dilated cardiomyopathy. *Circulation* 76(5), 1067–1073 (1987).

43 Allison JW, Barr LL, Massoth RJ, Berg GP, Krasner BH, Garra BS: Understanding the process of quantitative ultrasonic tissue characterization. *Radiographics* 14(5), 1099–1108 (1994).

44 Takiuchi S, Rakugi H, Honda K *et al.*: Quantitative ultrasonic tissue characterization can identify high-risk atherosclerotic alteration in human carotid arteries. *Circulation* 102(7), 766–770 (2000).

45 Kovacs A, Courtois MR, Weinheimer CJ *et al.*: Ultrasonic tissue characterization of the mouse myocardium: successful *in vivo* cyclic variation measurements. *J. Am. Soc. Echocardiogr.* 17(8), 883–892 (2004).

46 Oelze ML, O'Brien WD Jr, Blue JP, Zachary JF: Differentiation and characterization of rat mammary fibroadenomas and 4t1 mouse carcinomas using quantitative ultrasound imaging. *IEEE Trans. Med. Imaging* 23(6), 764–771 (2004).

▪ **Demonstrates the capabilities of quantitative ultrasound to differentiate benign from malignant growths using tumors from freshly killed mice.**

47 Mamou J, Oelze ML, O'Brien WD Jr, Zachary JF: Identifying ultrasonic scattering sites from three-dimensional impedance maps. *J. Acoust. Soc. Am.* 117(1), 413–423 (2005).

48 Foster FS, Pavlin CJ, Harasiewicz KA, Christopher DA, Turnbull DH: Advances in ultrasound biomicroscopy. *Ultrasound Med. Biol.* 26(1), 1–27 (2000).

49 Kolios MC: Biomedical ultrasound imaging: from 1 to 1000 mhz. *Can. Acoust.* 37(3), 35–42 (2009).

50 Le Floc'h J, Cherin E, Zhang MY *et al.*: Developmental changes in integrated ultrasound backscatter from embryonic blood *in vivo* in mice at high us frequency. *Ultrasound Med. Biol.* 30(10), 1307–1319 (2004).

51 Greenleaf JF, Sehgal CM: *Biologic System Evaluation with Ultrasound.* Springer-Verlag, NY, USA (1992).

52 Szabo TL: *Diagnostic Ultrasound Imaging: Inside Out.* Elsevier/Academic Press, Boston, MA, USA (2004).

53 Falou O, Kumaradas JC, Kolios MC: Finite-element modeling of elastic surface modes and scattering from spherical objects. *Proceedings of the COMSOL Conference.* Boston, MA, USA, 4–6 October 2007.

54 Morse PM, Ingard KU: *Theoretical Acoustics.* McGraw-Hill, NY, USA (1968).

55 Ratan KS, Subodh KS: Validity of a modified born approximation for a pulsed plane wave in acoustic scattering problems. *Phys. Med. Biol.* (12), 2823 (2005).

56 Insana MF: Modeling acoustic backscatter from kidney microstructure using an anisotropic correlation function. *J. Acoust. Soc. Am.* 97(1), 649–655 (1995).

57 Oelze Ml, O'Brien WD Jr: Method of improved scatterer size estimation and application to parametric imaging using ultrasound. *J. Acoust. Soc. Am.* 112(6), 3053–3063 (2002).

58 Kolios MC, Czarnota GJ: New insights into high frequency ultrasonic tissue scattering. Presented at: *3rd International Symposium on Medical, Bio- and Nano-Electronics.* Melbourne, Australia, 24–27 March 2008.

59 Goodman JW: Some fundamental properties of speckle. *J. Opt. Soc. Am.* 66(11), 1145–1150 (1976).

60 Wagner RF, Insana MF, Smith SW: Fundamental correlation lengths of coherent speckle in medical ultrasonic images. *IEEE Trans. Ultrason. Ferroelectr. Freq. Control* 35(1), 34–44 (1988).

61 Smith SW, Trahey GE, Hubbard SM, Wagner RF: Properties of acoustical speckle in the presence of phase aberration. Part II: correlation lengths. *Ultrason. Imaging* 10(1), 29–51 (1988).

62 Cotter TG: Apoptosis and cancer: the genesis of a research field. *Nat. Rev. Cancer* 9(7), 501–507 (2009).

63 Braunhut SJ, McIntosh D, Vorotnikova E, Zhou T, Marx KA: Detection of apoptosis and drug resistance of human breast cancer cells to taxane treatments using quartz crystal microbalance biosensor technology. *Ultrasound Med. Biol.* 3(1), 77–88 (2005).

64 Tsai MA, Waugh RE, Keng PC: Passive mechanical behavior of human neutrophils: effects of colchicine and paclitaxel. *Biophys. J.* 74, 3282–3291 (1998).

65 Weihs D, Mason TG, Teitell MA: Bio-microrheology: a frontier in microrheology. *Biophys. J.* 91, 4296–4305 (2006).

66 Mason TG, Ganesan K, Van Zanten JH, Wirtz D, Kuo SC: Particle tracking microrheology of complex fluids. *Phys. Rev. Lett.* 79, 3282–3285 (1997).

67 Girard KD, Chaney C, Delannoy M, Kuo SC, Robinson DN: Dynacortin contributes to cortical viscoelasticity and helps define the shape changes of cytokinesis. *EMBO J.* 23, 1536–1546 (2004).

68 El Kaffas A: Measuring the mechanical properties of apoptotic cells using particle tracking microrheology. Physics MSc Thesis, Ryerson University, ON, Canada (2008).

69 Czarnota GJ, Kolios MC, Sherar MD, Ottensmeyer FP, Hunt JW: High-frequency ultrasound imaging of apoptosis *in vitro*, *in situ*, and *in vivo*. *FASEB J.* 13(7), A1436 (1999).

70 Vlad R: Quantitative ultrasound characterization of responses to radiotherapy *in vitro* and *in vivo*. Medical Biophysics PhD Thesis, University of Toronto, ON, Canada(2009).

71 Brindle K: New approaches for imaging tumor responses to treatment. *Nat. Rev. Cancer* 8, 94–107 (2008).

▪▪ **Thorough review of modern imaging methods for tumor response detection spanning many extant imaging modalities and newer methods still under development.**

72 Blankenberg FG: *In vivo* detection of apoptosis. *J. Nucl. Med.* 49(Suppl. 2), S81–S95 (2008).

73 Patterson DM, Padhani AR, Collins DJ: Technology insight: water diffusion MRI – a potential new biomarker of response to cancer therapy. *Nat. Clin. Pract. Oncol.* 5, 220–233 (2008).

74 Krishnan AS, Neves AA, de Backer MM *et al.*: Detection of cell death in tumors by using MR imaging and a gadolinium-based targeted contrast agent. *Radiology* 246, 854–862 (2008).

75 Sharma R, Katz JK: Taxotere chemosensitivity evaluation in mice prostate tumor: validation and diagnostic accuracy of quantitative measurement of tumor characteristics by MRI, PET, and histology of mouse tumors. *Technol. Cancer Res. Treat.* 7, 175–186 (2008).

76 Sierra A, Michaeli S, Niskanen JP *et al.*: Water spin dynamics during apoptotic cell death in glioma gene therapy probed by T1rho and T2rho. *Magn. Reson. Med.* 59, 1311–1319 (2008).

77 Tseng Y, Lee JS, Kole TP, Jiang I, Wirtz D: Micro-organization and visco-elasticity of the interphase nucleus revealed by particle nanotracking. *J. Cell. Sci.* 117(Pt 10), 2159–2167 (2004).

78 Brand S, Weiss EC, Lemor RM, Kolios MC: High frequency ultrasound tissue characterization and acoustic microscopy of intracellular changes. *Ultrasound Med. Biol.* 34(9), 1396–1407 (2008).

79 Strohm E, Kolios MC: Quantifying ultrasonic properties of cells during apoptosis using time resolved acoustic microscopy. Presented at: *IEEE International Ultrasonics Symposium*. Rome, Italy, 19–23 September 2009.

80 Sarvazyan AP, Hill CR: Physical chemistry of the ultrasound-tissue interaction. In: *Physical Principles of Medical Ultrasonics.* Hill CR, Bamber JC, Ter Haar GR (Eds). John Wiley & Sons, UK (2004).

81 Falou O, Kumaradas JC, Kolios MC: Finite-element modeling of acoustic wave scattering from fluid, rigid and elastic objects. *Can. Acoust.* 33(3), 84–85 (2005).

82 Hunt JW, Worthington AE, Kerr AT: The subtleties of ultrasound images of an ensemble of cells: simulation from regular and more random distributions of scatterers. *Ultrasound Med. Biol.* 21(3), 329–341 (1995).

83 Hunt JW, Worthington AE, Xuan A, Kolios MC, Czarnota GJ, Sherar MD: A model based upon pseudo regular spacing of cells combined with the randomisation of the nuclei can explain the significant changes in high-frequency ultrasound signals during apoptosis. *Ultrasound Med. Biol.* 28(2), 217–226 (2002).